THE JOURNAL OF BIOLOGICAL CHEMISTRY VOL. 288, NO. 39, pp. 27812–27824, September 27, 2013

Dynein Interacts with the Neural Cell Adhesion Molecule (NCAM180) to Tether Dynamic Microtubules and Maintain Synaptic Density in Cortical Neurons*[S]

Received for publication, February 26, 2013, and in revised form, August 14, 2013 Published, JBC Papers in Press, August 19, 2013, DOI 10.1074/jbc.M113.465088

Eran Perlson[‡§1], Adam G. Hendricks[¶1], Jacob E. Lazarus[¶], Keren Ben-Yaakov[‡§], Tal Gradus[‡§], Mariko Tokito[¶], and Erika L. F. Holzbaur[¶2]

From the [‡]Department of Physiology and Pharmacology, Sackler Faculty of Medicine, and the [§]Sagol School of Neuroscience, Tel Aviv University, Tel Aviv 69978, Israel and the [¶]Department of Physiology and the Pennsylvania Muscle Institute, Perelman School of Medicine, University of Pennsylvania, Philadelphia, Pennsylvania 19104-6085

Background: Dynein is a microtubule motor that can also tether dynamic microtubule plus-ends.
Results: Neural cell adhesion molecule isoform-180 (NCAM180) binds directly to dynein, facilitating microtubule tethering at the cortex and enhancing cell-cell adhesion and synaptic density.
Conclusion: The dynein-NCAM180 interaction contributes to the maintenance of synaptic density in cortical neurons.
Significance: Dynein functions as both microtubule motor and microtubule tether in neurons.

Cytoplasmic dynein is well characterized as an organelle motor, but dynein also acts to tether and stabilize dynamic microtubule plus-ends *in vitro*. Here we identify a novel and direct interaction between dynein and the 180-kDa isoform of the neural cell adhesion molecule (NCAM). Optical trapping experiments indicate that dynein bound to beads via the NCAM180 interaction domain can tether projecting microtubule plus-ends. Live cell assays indicate that the NCAM180-dependent recruitment of dynein to the cortex leads to the selective stabilization of microtubules projecting to NCAM180 patches at the cell periphery. The dynein-NCAM180 interaction also enhances cell-cell adhesion in heterologous cell assays. Dynein and NCAM180 co-precipitate from mouse brain extract and from synaptosomal fractions, consistent with an endogenous interaction in neurons. Thus, we examined microtubule dynamics and synaptic density in primary cortical neurons. We find that depletion of NCAM, inhibition of the dynein-NCAM180 interaction, or dampening of microtubule dynamics with low dose nocodazole all result in significantly decreased in synaptic density. Based on these observations, we propose a working model for the role of dynein at the synapse, in which the anchoring of the motor to the cortex via binding to an adhesion molecule mediates the tethering of dynamic microtubule plus-ends to potentiate synaptic stabilization.

Cytoplasmic dynein is a multisubunit molecular motor that moves processively toward the minus-ends of microtubules. Dynein drives the motility of organelles, vesicles, proteins, and RNA particles and is also essential for spindle assembly and dynamics during cell division (1), making dynein critical for normal cellular function in higher eukaryotes. The diverse functions of dynein in the cell are probably coordinated through specific protein-protein interactions, many of which are mediated by the dynein intermediate chain, which is localized at the base of the motor complex and interacts with critical binding partners, such as dynactin (1, 2).

Dynein interacts with the dynamic microtubule cytoskeleton. Microtubules undergo periods of growth and shrinkage due to the addition and loss of tubulin subunits, primarily at their plus-ends. These dynamics allow microtubule plus-ends to explore cellular space. A "search-and-capture" hypothesis has been proposed, stating that microtubule plus-ends can be preferentially captured and stabilized through productive interactions with organelles or the cell cortex (3). This stabilization may promote the selective anchoring of microtubule plus-ends at the cortex, leading to cell polarization or targeted trafficking to specific cellular domains (4).

Strong evidence that cortically localized dynein can mediate interactions between microtubules and the cell periphery comes from budding yeast, where dynein's primary role is to exert tension on microtubules projecting from the spindle pole body in order to properly position the nucleus (5–8). A parallel mechanism has been proposed for higher eukaryotes because cortically localized dynein has been implicated in the proper positioning of the spindle in dividing cells (9, 10). Cortically localized dynein has also been suggested to mediate microtubule capture and tethering in interphase cells, primarily at sites of cell-cell interaction, such as adherens junctions (11, 12) and the immunological synapse (13).

Recent biophysical studies have modeled the interaction of projecting microtubules with cortically localized dynein *in vitro*. Purified mammalian dynein motors bound to beads were found to tether and stabilize projecting microtubule plus-ends, delaying microtubule depolymerization in an ATP-dependent

* This work was supported, in whole or in part, by National Institutes of Health (NIH) Grant NS060698 (to E. L. F. H.), an NIH postdoctoral fellowship (to A. G. H.), and an NIH predoctoral fellowship (to J. E. L.). This work was also supported by a Muscular Dystrophy Association Postdoctoral Fellowship and Israel Science Foundation Grant 060116480 (to E. P.).
[S] This article contains supplemental Videos 1–3.
[1] Both authors contributed equally to this work.
[2] To whom correspondence should be addressed: Dept. of Physiology, University of Pennsylvania Perelman School of Medicine, 630 Clinical Research Bldg., 415 Curie Blvd., Philadelphia, PA 19104-6085. Tel.: 215-573-3257; Fax: 215-573-5851; E-mail: holzbaur@mail.med.upenn.edu.

manner (14). Similarly, recombinant yeast dynein bound to a rigid barrier also tethered microtubule plus-ends and promoted the formation of stable attachments with the barrier (15). Thus, biophysical studies support the hypothesis that dynein can act as either a motor or a tether. However, the mechanisms that specifically localize dynein to the cortex are still not well understood, especially in interphase mammalian cells.

Here, we identify a novel interaction between dynein intermediate chain (DIC)[3] and the neural cell adhesion molecule NCAM180. NCAM is a transmembrane protein that is localized to synaptic sites (16, 17), mediates intercellular interactions across the synapse, and is important for synaptic maturation, plasticity, and stabilization (18–24). Three major isoforms of NCAM are generated by alternative splicing (NCAM180, NCAM140, and NCAM120), which differ in their membrane association and intracellular domains (25, 26). Loss of the NCAM180 isoform leads to alterations in synaptic morphology as well as function (27).

We find that the dynein-NCAM180 interaction is direct and specific. Binding to NCAM180 recruits dynein to the cortex and leads to the plus-end tethering of microtubules at NCAM180 patches at the cell periphery in a heterologous cell system. In cortical neurons, disruption of the endogenous dynein-NCAM180 interaction alters microtubule dynamics at the synapse and leads to a decrease in synaptic density. Together, these observations support a model in which dynein, localized to the cell cortex through a direct association with NCAM180, mediates microtubule tethering and contributes to the maintenance of synaptic stability in neurons.

EXPERIMENTAL PROCEDURES

Yeast Two-hybrid Assay—A yeast two-hybrid assay was performed using full-length DIC1 to screen a random-primed human fetal brain cDNA library, leading to detection of a cDNA clone encoding residues 975–1105 of NCAM180 (EAW67201.1, neural cell adhesion molecule 1, isoform CRA_a).

Plasmids and Constructs—Bacterial expression vector pET-DIC1 expressing His-tagged full-length DIC1 was described previously (28); the sequence encoding residues 971–1105 in human NCAM180 was subcloned from the yeast two-hybrid clone into pGEX-6P2 to generate pGEX-DBS. Mammalian expression plasmids encoding GFP-NCAM120, cyan fluorescent protein-NCAM140, cyan fluorescent protein-NCAM180, and RFP-NCAM180 in the pcDNA3.19 vector were a gift from Lynn Landmesser. GFP-NCAM180ΔDBS, a C-terminal deletion construct of NCAM180 lacking residues 971–1115, and GFP-DBS, with NCAM180 residues 971–1105 fused to GFP, were subcloned by PCR from the Landmesser cDNA clones; a parallel construct expressing blue fluorescent protein-DBS was also generated. GFP-CC1 encodes residues 216–550 of human $p150^{Glued}$ in a mammalian cell expression vector (29). EB3 labeled at the C terminus with mCherry (EB3-mCherry) was provided by I. Kaverina (30), 3xGFP-EMTB was a gift of Chloe Bulinski (31), and GFP-Bsn (32) was a gift from the Gundelfinger laboratory.

Antibodies for Western Blotting and Immunofluorescence—Antibodies to DIC (MAB1618) and PSD95 (MAB1596) were from Chemicon. Synapsin antibody (AB1543P) was from Millipore. Antibodies to dynactin subunits p150 (610474) and p50 (611003) and to NCAM (556324 and 556323) were from BD Transduction Laboratories. GAPDH antibody (ab9484) was from Abcam. Chicken GFP antibody (GFP-1020) was from Aves Labs, Inc. Rabbit polyclonal antibodies UP1467 to DIC and UP502 and UP1097 to dynactin subunits $p150^{Glued}$ and p50 were generated and affinity-purified in our laboratory.

Protein Purification—Cytoplasmic dynein and tubulin were purified from bovine brain as described (33, 34). Labeled tubulin was purchased from Cytoskeleton, Inc. Recombinant DIC was purified as described (28). GST and GST fusion proteins were purified as described (35).

Pull-down Assays—His-tagged recombinant DIC was used for *in vitro* GST-NCAM pull-down assays or was coupled to activated CH-Sepharose 4B beads for DIC pull-down assays (36). Mouse brain homogenate in 1% Triton, PBS with protease and phosphatase inhibitors from Roche Applied Science (homogenization buffer) was centrifuged at low speed to obtain brain extract and then precleared by incubation with BSA-bound CH-Sepharose 4B beads. Following incubation in precleared extract for 2 h, DIC beads were washed and eluted by boiling in SDS sample buffer for analysis by Western blot. For GST-DBS pull-down experiments, either GST-DBS fusion protein or purified GST was bound to glutathione beads. For NCAM immunoprecipitations, brain extract from age-matched young adult wild type mice homogenized in homogenization buffer and precleared by incubation with "empty" Dynabeads (Millipore) for 1 h at 4 °C were incubated overnight with anti-NCAM antibody (catalog no. 556324, BD Biosciences) at a ratio of 1 mg of total protein to 2 μg of anti-NCAM antibody in 1 ml of buffer overnight at 4 °C. Dynabeads were added and incubated for 1 h at 4 °C, the beads were washed, and the bound proteins were eluted by boiling in gel sample buffer. The resulting blots were probed with anti-DIC from Chemicon.

For microtubule pull-down assays, GST-DBS or GST control beads were incubated with BSA (10 μg/μl), washed, and incubated with or without purified dynein-dynactin in motility assay buffer (MAB; 10 mM PIPES, 50 mM potassium acetate, 4 mM $MgCl_2$, 1 mM EGTA, pH 7.0). Beads were then incubated with rhodamine-labeled microtubules, extensively washed, and analyzed by Western blot.

Optical Trap Tethering Assay—The tethering assay was performed as described (14), with slight modifications. A polyclonal antibody to GST (Invitrogen) was covalently conjugated to carboxylated 1-μm polystyrene beads (Polysciences, Inc.). Beads were then incubated with GST-DBS for 30 min on ice and washed two times and resuspended in MAB with 10 mg/ml BSA. Next, beads were incubated with dynein, purified from cow brain (33) for 30 min on ice, and washed and resuspended in MAB with 10 mg/ml BSA. The GST-DBS- and dynein-coated beads were diluted into MAB supplemented with 20 μM taxol, 1 mM DTT, 1 mM ATP, 10 mg/ml glucose, 1 μg/ml glu-

[3] The abbreviations used are: DIC, dynein intermediate chain; DHC, dynein heavy chain; NCAM, neural cell adhesion molecule; DBS, dynein-binding site; MAB, motility assay buffer; DIV, days *in vitro*; ANOVA, analysis of variance; NMJ, neuromuscular junction; RFP, red fluorescent protein.

cose oxidase, and 0.5 μg/ml catalase and introduced into the sample chamber; imaging and data analysis were performed as described (14).

Cell Culture and Transfection—COS7 cells from ATCC and HeLa cells stably expressing DHC-GFP (10), generously provided by the Hyman (Max Planck Institute) and Cheeseman (Whitehead Institute) laboratories, were transiently transfected using Fugene 6 (Roche Applied Science) according to the manufacturer's instructions. Cortical neurons were isolated from embryonic day 19 Sprague-Dawley rat embryos or postnatal day 0 mice (37). Dissociated cells were cultured for 5–14 days *in vitro* (DIV) as noted with serum-free Neurobasal medium (Invitrogen) supplemented with B27 (Invitrogen). Neurons were transfected prior to plating using an Amaxa Nucleofector system (Lonza) according to the manufacturer's recommendations.

Knockdown of endogenous NCAM in cortical neurons isolated from mouse was performed by lentiviral infection, using recombinant lentiviruses expressing GFP or shRNA against NCAM from Sigma (shRNA1, CCGGC GTGCC CATTC TCAAG TACAA CTCGA GTTGT ACTTG AGAAT GGGCA CGTTT TTG; shRNA2, CCGGC GTTGG AGAGT CCAAA TTCTT CTCGA GAAGAA TTTGG ACTCT CCAAC GTTTT TG; shRNA3, CCGGC CAAGC TCCAA CTACA GCAAT CTCGA GATTG CTGTA GTTGG AGCTT GGTTT TTG; shRNA4, CCGGC GTGCC CATTC TCAAG TACAA CTCGA GTTGT ACTTG AGAAT GGGCA CGTTT TTG). Lentiviral vectors pHR-GFP, pLV-VSVG, and pLVdeltaR8.2 were a gift from Dr. Eran Bachrach (Tel Aviv University); lentivirus was produced by transient transfection in HEK293T cells as described (38). Neurons were infected with lentiviruses 1 day after plating. At 14 DIV, cells were harvested for protein extraction and Western blot analysis or fixed with 4% paraformaldehyde and immunostained for synapsin, neurofilament-H, and PSD-95.

Aggregation Assays—Aggregation was assayed as described (39), 18 h after transfection of COS7 cells with the indicated constructs; incubations with nocodazole were performed as noted with either 10 μM (high dose) or 100 nM (low dose) at 37 °C for 40 min. Total cell number and number of cells in aggregates (defined as >5 cells each) were counted; the percentage of total cells in aggregates was calculated relative to controls.

Imaging of Microtubule Dynamics—To image microtubule dynamics in COS7 cells, the cells were transfected with 3xGFP-EMTB using Fugene6 (Roche Applied Science) and imaged 1 day later in glass bottom microwell dishes (Fluorodish, World Precision Instruments) containing Hibernate-A low fluorescence medium (Invitrogen) at 37 °C. Imaging was performed using a Leica DMI6000B microscope and a Hamamatsu C10600 Orca-R2 camera. Images were acquired every 3–6 s with a ×100 objective.

Microtubule dynamics were measured in cortical neurons isolated from E19 Sprague-Dawley rat embryos and transfected using an Amaxa nucleofector system (Lonza) on the day of plating. Neurons were imaged at 7 DIV using total internal reflection fluorescence microscopy. First, static images of GFP-synaptophysin and blue fluorescent protein-DBS were acquired. Then EB3-mCherry dynamics were imaged at 2 frames/s for 500 frames. To produce kymographs of EB3 dynamics, reference lines were drawn along EB3 comet trajectories using a maximum projection image as a guide. Using the same reference lines that were used to produce the EB3 kymographs, line scans were taken of GFP-synaptophysin fluorescence. The start and end point of each EB3 comet was manually tracked. Synapses were identified automatically from line scans of GPF-synaptophysin as areas of intensity above a threshold set to the 25th quantile. These data were used to calculate the fraction of comets that terminated at a synapse, the fraction of neurite length positive for GFP-synaptophysin, the average velocity of EB3 comets, and the apparent catastrophe frequency of microtubules (the reciprocal of the EB3 comet duration).

Synaptic Membrane Preparation—Isolation of synaptic membranes was adapted from Ref. 40. Briefly, brain tissue from four mice (~1.6 g) was homogenized in 20 ml of cold dissection buffer (50 mM Tris acetate, pH 7.4, 10% sucrose, 5 mM EDTA, with protease inhibitors) and then centrifuged first at 800 × *g* for 20 min and then at 16,000 × *g* for 30 min. The resulting pellet was resuspended in 10 ml of 20 mM HEPES buffer, pH 7.4, and centrifuged again at 16,000 × *g* for 15 min. The pellet was resuspended in lysis buffer (5 mM Tris, pH 8.1; protease inhibitors) and incubated on ice for 45 min. Synaptosomes were isolated from a three-step sucrose gradient centrifuged at 60,000 × *g* for 2 h; the band at the 28.5 and 34% sucrose interface was collected.

Analysis of Synaptic Colocalization and Synaptic Density—Cortical neurons from mice, 14 DIV, were fixed and stained for synapsin, dynein, and NCAM or PSD-95. Approximately 10 random fields for each condition were imaged using fluorescence microscopy at ×100 magnification and analyzed with Imaris colocalization software (Bitplane) as described (41). Synaptic density was scored as either the apposition of presynaptic and postsynaptic markers along the processes of cortical neurons using antibodies to synapsin-1 and PSD95 or by the uptake of FM4-64 upon K^+ stimulation. FM4-64 labeling of active synapses was performed as described (42). Cortical neurons were grown for 12 days and then exposed to 10 μM FM4-64 for 2 min in 31.5 mM NaCl, 90 mM KCl, 5 mM Hepes, 1 mM $MgCl_2$, 2 mM $CaCl_2$, 30 mM glucose; washed three times with Hibernate-A low fluorescence buffer with 50 μM DL-2-amino-5-phosphonopentanoic acid and 10 μM 6,7-dinitroquinoxaline-2,3-dione; and then either imaged live or fixed and imaged.

RESULTS

Identification of a Direct and Specific Interaction between Dynein and NCAM180—We performed a yeast two-hybrid screen from a fetal human brain cDNA library for novel dynein interactors, using the neuron-specific isoform DIC1A as bait and identified the intracellular domain of NCAM (residues 975–1105) as a binding partner. Only the NCAM180 isoform encodes the dynein-binding site (DBS) identified in the yeast two-hybrid assay (Fig. 1*A*). To confirm this observation, we performed *in vitro* pull-down assays using purified recombinant DIC1 and either GST fused to the DBS of NCAM180 or GST only as a control. We observed specific binding of DIC1 to the DBS of NCAM180 (Fig. 1, *B–E*). GST-DBS pull-down

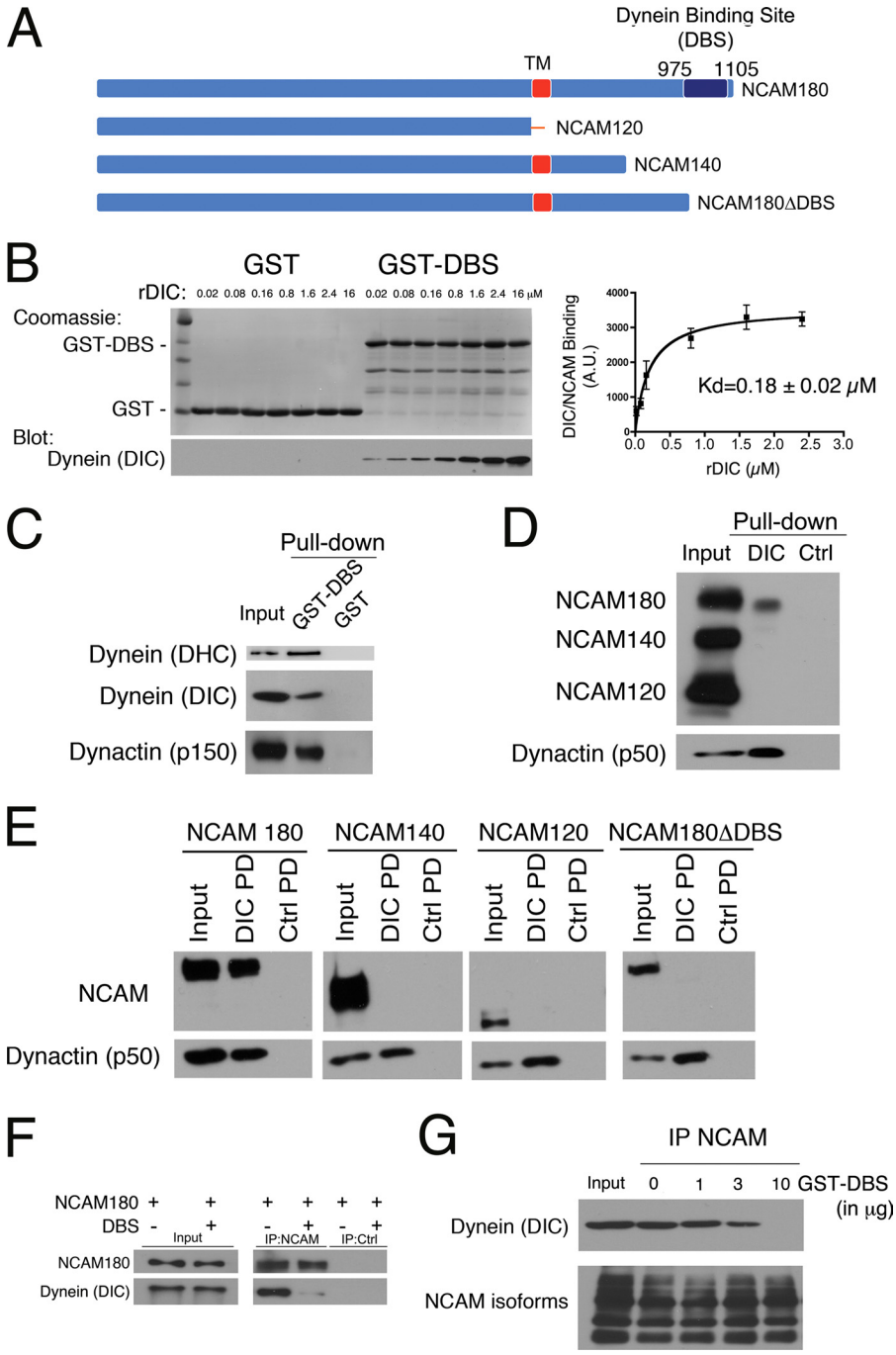

FIGURE 1. **A direct interaction between dynein and NCAM180 recruits dynein to the cell cortex.** *A*, three major isoforms of NCAM are expressed in mammalian neurons: NCAM180, NCAM140, and NCAM120. The DBS identified in the yeast two-hybrid screen, spanning residues 975–1105 of NCAM180, is shown. *TM*, transmembrane domain. *B*, direct binding of recombinant DIC to the DBS domain of NCAM180. Pull-down assays were performed with either GST or GST-DBS incubated with increasing concentrations of purified recombinant DIC (*rDIC*), as noted. GST-DBS and recombinant DIC bind with an apparent K_d of 0.18 ± 0.02 μM. *C*, dynein and dynactin are precipitated from mouse brain lysate by recombinant GST-DBS but not by GST. *Input*, 10% of total; Western blots were probed with antibodies to DHC, DIC, and dynactin ($p150^{Glued}$ subunit). *D*, dynein interacts specifically with NCAM180. NCAM180, but not NCAM140 or NCAM120, was precipitated from mouse brain extract with recombinant DIC bound to beads. Dynactin (p50 subunit) served as a positive control, and BSA control beads served as a negative control. *Input*, 10% of total. *E*, DIC pull-down (*PD*) experiments from COS7 cells transfected with mouse isoforms NCAM180, NCAM140, NCAM120, or with a construct lacking the dynein-binding site, NCAM180ΔDBS, demonstrate the specificity of the dynein-NCAM180 interaction and its dependence on the DBS domain. Input (10% of total), DIC pull-down (*DIC PD*), and BSA control pull-down (*Ctrl PD*) samples were probed with antibodies to NCAM; dynactin (*p50*) served as a positive control. *F*, co-expression of the DBS construct disrupts the co-immunoprecipitation of endogenous dynein with NCAM180 from COS7 cells; a control immunoprecipitation with protein A beads alone (*IP:Ctrl*) is also shown. *G*, disruption of the dynein-NCAM180 interaction is dose-dependent. The co-immunoprecipitation (*IP*) of endogenous dynein with NCAM from brain lysate is inhibited by the addition of purified recombinant GST-DBS (0, 1, 3, and 10 μg of DBS to 1 mg of total protein in lysate). *Input*, 10% of total. *Error bars*, S.E.

experiments performed over a range of recombinant DIC concentrations indicate an apparent dissociation constant (K_d) of 0.18 ± 0.02 μM (Fig. 1*B*), consistent with a physiologically relevant interaction. The specificity of the dynein-NCAM180 interaction is further supported by precipitation of endogenous proteins from brain lysate. Dynein heavy chain (DHC), DIC,

and dynactin (p150) were precipitated with GST-DBS bound to beads but not by control GST-bound beads (Fig. 1*C*). In the reciprocal experiment, endogenous NCAM180 was precipitated from brain lysate by recombinant DIC1-bound beads but not by control beads. Neither the NCAM140 nor the NCAM120 isoforms that lack the DBS domain identified in the yeast two-hybrid screen were precipitated by DIC-bound beads in this assay (Fig. 1*D*).

To further test the specificity of the dynein-NCAM180 interaction, we used COS7 cells, which do not express endogenous NCAM. COS7 cells were singly transfected with each of the major NCAM isoforms: NCAM180, NCAM140, or NCAM120. Only the NCAM180 isoform was precipitated from COS7 cell lysate with DIC-bound beads (Fig. 1*E*); neither the NCAM140 nor NCAM120 isoforms were precipitated with DIC-bound beads, and no NCAM binding to control beads was observed. We also expressed a C-terminal truncation of NCAM180 lacking the DBS domain (NCAM180ΔDBS) in COS7 cells and found that the NCAM180ΔDBS construct was not precipitated by DIC-bound beads (Fig. 1*E*). Together with the direct binding assay described above, these data indicate that the DBS domain in NCAM180 is both necessary and sufficient for binding to DIC (Fig. 1, *B–E*).

Next, we used an anti-NCAM antibody to immunoprecipitate NCAM180 from COS7 cells either transiently transfected with NCAM180 alone or co-transfected with NCAM180 and the DBS domain. We found that co-expression of the DBS domain dominantly inhibited the co-immunoprecipitation of dynein with NCAM180 (Fig. 1*F*). This dominant inhibition of the dynein-NCAM180 binding interaction is dose-dependent, because the addition of increasing concentrations of recombinant DBS effectively blocked the co-immunoprecipitation of dynein with NCAM antibodies from brain lysate (Fig. 1*G*). Thus, the dynein-binding domain we have identified in the C-terminal intracellular tail of NCAM180 mediates the direct and specific binding of dynein to NCAM180, whereas overexpression of the DBS domain results in a dominant negative inhibition of the dynein-NCAM180 interaction.

NCAM180-dependent Recruitment of Dynein to the Cortex Leads to the Selective Tethering of Projecting Microtubule Plus-ends—We have previously found that dynein immobilized on beads can tether and stabilize dynamic microtubule plus-ends *in vitro* (14). We asked whether dynein, anchored to a bead by NCAM180, would have a similar activity. We covalently coupled anti-GST antibody to beads and then bound either purified recombinant GST-DBS or purified GST as a control. We incubated the beads with microtubules in the absence and presence of dynein. We found that GST-DBS beads bound to both dynein and microtubules, as assessed by Western blot (Fig. 2*A*). In the absence of dynein, no association of microtubules with GST-DBS beads was observed, and in the absence of GST-DBS, neither dynein nor microtubules bound to beads. Next, we asked whether dynein, bound to beads through GST-DBS, could tether microtubule plus-ends. We used an optical trap to position DBS- and dynein-bound beads near the laterally diffusing ends of Taxol-stabilized microtubules as described (14) and imaged the effects of the resulting interaction on the diffusion of the microtubule end. We found that dynein anchored to beads via the DBS domain of NCAM180 was capable of capturing and stabilizing projecting microtubule plus-ends, substantially reducing lateral diffusion (Fig. 2*B*). When tethered to the DBS- and dynein-bound beads, the variance of the lateral position of the microtubule was $0.012 \pm 0.05\ nm^2$, compared with a value of $1.23 \pm 1.13\ nm^2$ observed for control beads coated with BSA. These results show that dynein recruited by NCAM180 can tether microtubule plus-ends in a minimal system.

To examine the cellular effects of the dynein-NCAM180 interaction, we expressed the NCAM180 in COS7 cells, which do not normally express this protein (Fig. 2*C*). We observed that heterologous expression of NCAM180 was sufficient to recruit dynein to the plasma membrane. In untransfected COS7 cells, dynein was found in a punctate pattern throughout the cell but was not localized to the plasma membrane; there is also some nonspecific labeling of the nucleus by the dynein antibody in both control and transfected cells. In COS7 cells transfected with NCAM180, we observed the recruitment of dynein to the plasma membrane (Fig. 2*C*); this cortical localization is not seen in untransfected control cells. As shown above (Fig. 1, *F* and *G*), the DBS domain of NCAM180 acts as a dominant negative inhibitor of the dynein-NCAM180 interaction *in vitro*. Consistent with these data, we found that expression of the DBS domain in cells blocked the recruitment of dynein to the cortex induced by NCAM180 expression (Fig. 2*C*).

To further investigate this cortical recruitment, we used a HeLa cell line stably expressing dynein heavy chain with a C-terminal GFP tag (DHC-GFP) (10). In control interphase cells, we see dynein distributed throughout the cytoplasm but no enrichment at the cortex (Fig. 2*D*). However, heterologous expression of NCAM180 leads to the formation of patches at the cortex (see *arrows* in Fig. 1*D*, *bottom row*), and we find that DHC-GFP is recruited to these patches.

Of note, the recruitment of dynein to the plasma membrane induced by the heterologous expression of NCAM180 in COS7 or HeLa cells is distinct from the dominant relocalization of cellular dynein induced by expression of the N-terminal domain of BICD2, which acts as a general dominant negative inhibitor of dynein function *in vivo* (43). Although expression of NCAM180 appears to be sufficient to recruit dynein to the cortex, it does not generally inhibit dynein-mediated intracellular motility because we did not observe disruption of steady state organelle localization, such as that induced by expression of the dominant negative CC1 construct of dynactin (44). Also, when expressed in cortical neurons, the DBS construct does not disrupt the dynein-driven motility of late endosomes and lysosomes visualized with Lysotracker or the transport of Bassoon transport vesicles visualized with the GFP-Bsn reporter (32) (data not shown). These observations suggest that expression of the DBS construct results in a specific inhibition of the dynein-NCAM180 interaction but not other dynein-mediated functions, including axonal transport.

To examine the effects of the NCAM180-induced recruitment of dynein to the cortex on the microtubule cytoskeleton, we imaged microtubule dynamics in COS7 cells expressing NCAM180 using GFP-EMTB, a well characterized reporter for microtubule dynamics in live cells (31). In control cells, we observed robust microtubule dynamics, characterized by slow

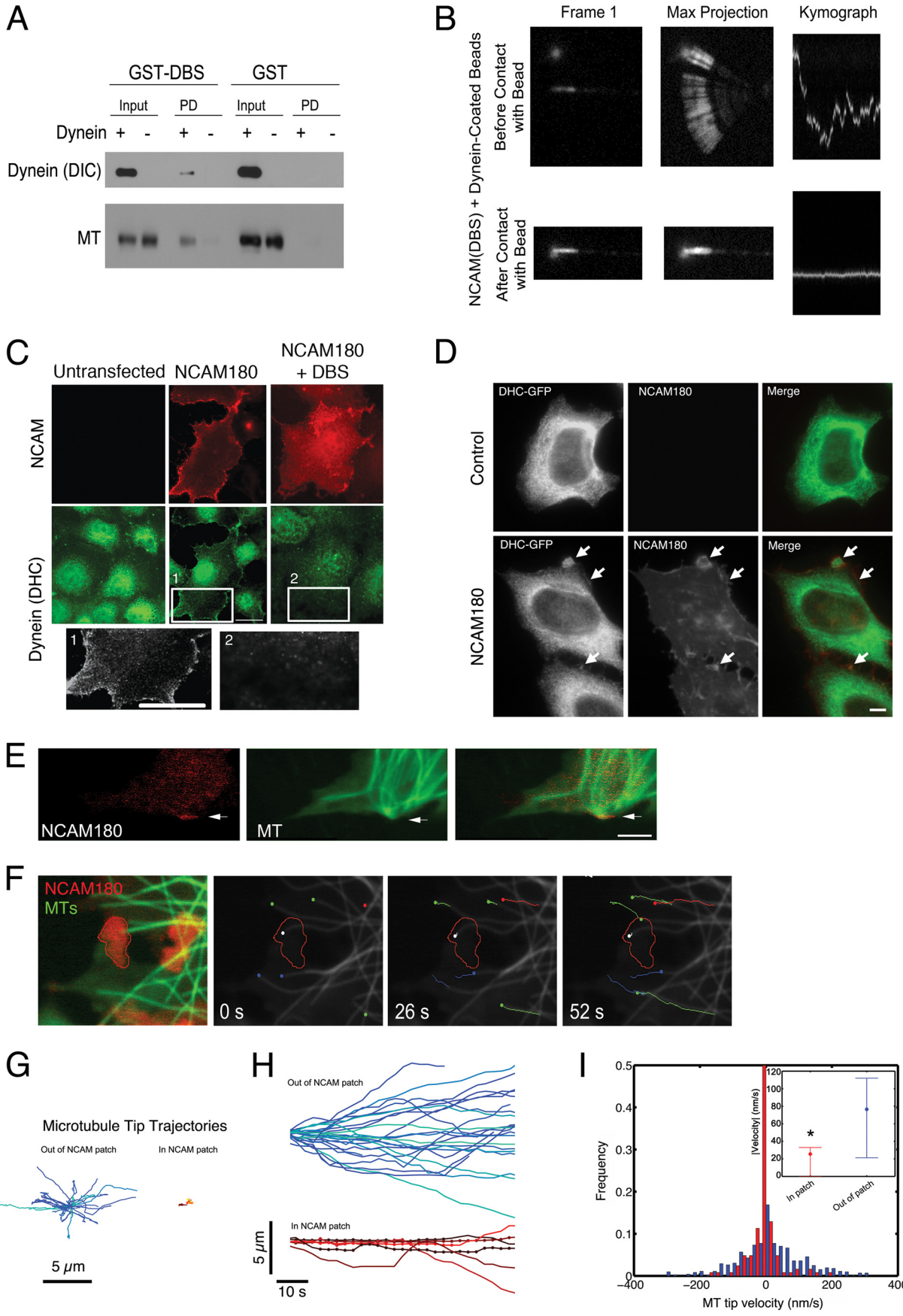
A
GST-DBS
GST
Input
PD
Input
PD
Dynein + - + - + - + -
Dynein (DIC)
MT
B
Frame 1
Max Projection
Kymograph
NCAM(DBS) + Dynein-Coated Beads
Before Contact with Bead
After Contact with Bead
C
Untransfected
NCAM180
NCAM180 + DBS
NCAM
Dynein (DHC)
1
2
1
2
D
DHC-GFP
NCAM180
Merge
Control
NCAM180
E
NCAM180
MT
F
NCAM180
MTs
0 s
26 s
52 s
G
Microtubule Tip Trajectories
Out of NCAM patch
In NCAM patch
5 μm
H
Out of NCAM patch
In NCAM patch
5 μm
10 s
I
Frequency
MT tip velocity (nm/s)
|Velocity| (nm/s)
In patch
Out of patch
*

growth and rapid shrinkage, leading to the efficient exploration of the cellular space in the vicinity of the cortex (supplemental Video 1). Heterologous expression of RFP-NCAM180 leads to the formation of membrane-associated patches visible in live cell microscopy (Fig. 2*E*); immunocytochemistry shows that dynein is recruited to NCAM180 patches at the cell periphery (Fig. 2*C*). Expression of NCAM180 did not alter overall microtubule organization or dynamics. However, in live cell assays, we observed the apparent capture and tethering of those microtubule plus-ends that randomly projected to NCAM180 patches at the cortex (Fig. 2*E*).

We compared the dynamics of microtubules projecting into NCAM patches to the dynamics of microtubules projecting to regions of the cortex without visible RFP-NCAM180 (Fig. 2*F* and supplemental Videos 2 and 3). Microtubule plus-ends projecting into membrane-bound patches of NCAM180 showed dampened dynamics (Fig. 2, *G* and *H*), including a statistically significant decrease in microtubule tip velocities during growth and shortening ($p < 0.001$; Fig. 2*I*), relative to microtubule plus-ends away from NCAM180 patches at the cortex. These dampened dynamics were accompanied by an increased microtubule dwell time at the cortex. The average dwell time for microtubule plus-ends in the vicinity of NCAM patches was 189 ± 12 s, significantly greater than the 94 ± 15-s average dwell time for microtubules projecting into cortical areas of the same cells without visible NCAM localization or similar measurements in untransfected control cells (100 ± 7 s; $p < 0.01$).

The Dynein-NCAM180 Interaction Promotes Cell Adhesion—We hypothesized that the transient tethering of microtubules by dynein recruited to cortical patches by NCAM180 might lead to enhanced cell-cell adhesion. Using an established adhesion assay (39), we found that expression of NCAM180 in COS7 cells led to a significant increase in cell-cell association (282 ± 27% of GFP control, $p < 0.05$; Fig. 3, *A* and *B*) as compared with cells expressing NCAM lacking the dynein binding site (NCAM180ΔDBS, 111 ± 10% of GFP control). Co-expression of CC1, a well characterized dominant negative inhibitor of dynein function (44), suppressed the enhanced cell-cell adhesion induced by NCAM180 expression (168 ± 10%; $p < 0.05$), indicating that both NCAM180 and dynein are needed to promote cell-cell interactions (Fig. 3, *A* and *B*).

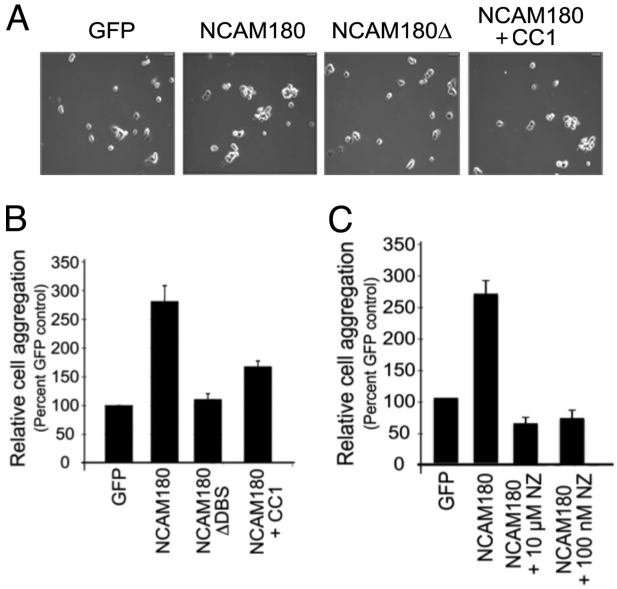

FIGURE 3. **Cell-cell interactions are dependent on microtubule dynamics and the dynein-NCAM interaction.** *A* and *B*, COS7 cells were singly transfected with GFP, NCAM180, or NCAMΔDBS or doubly transfected with NCAM180 and the dynein inhibitor CC1. The enhanced aggregation induced by NCAM180 ($p < 0.05$) was not seen when the DBS was deleted or when dynein was inhibited by co-expression of the dominant negative construct CC1 (44). *C*, COS7 cells were transfected with NCAM180 and then treated either with either low dose (100 nM) or high dose (10 μM) nocodazole for 40 min. The enhanced aggregation induced by NCAM180 expression was blocked by nocodazole treatment to either depolymerize cellular microtubules at high dose nocodazole or dampen microtubule dynamics at low dose nocodazole. The percentage of cells in aggregates was scored relative to control cells expressing GFP. *Error bars*, S.E. from ≥3 replicates.

We also found that the enhanced cell-cell adhesion induced by expression of NCAM180 is microtubule-dependent (Fig. 3*C*), because aggregation was not increased in cells transfected with NCAM180 and then treated with either high dose (10 μM) nocodazole to depolymerize microtubules or low dose (100 nM) nocodazole to dampen microtubule dynamics without depolymerizing the microtubule cytoskeleton (45).

The Dynein-NCAM180 Interaction Modulates Microtubule Dynamics in Cortical Neurons—Our observations in COS7 cells and *in vitro* reconstitution experiments indicate that dynein, anchored by binding to NCAM180, can tether project-

FIGURE 2. **NCAM180 and dynein tether microtubule plus-ends *in vitro* and in cells.** *A*, GST-DBS-bound beads or GST-bound control beads were incubated with purified microtubules in the presence (+) or absence (−) of dynein; binding was evaluated by Western blot with antibodies to dynein (*DIC*) and tubulin (*MT*). *Input*, 10% of total. Both dynein and microtubules bound to GST-DBS beads but not to control beads. *B*, an optical trap was used to position a DBS-dynein-bound bead near the diffusing plus-end of a microtubule, which was bound to the coverglass at its minus-end. A marked decrease in the lateral diffusion of the microtubule plus-end was observed after contact with the bead, as shown in both the maximum projection and the kymograph showing microtubule end dynamics over time. *C*, expression of exogenous NCAM180 in COS7 cells recruits dynein to the cell cortex (NCAM180). Co-expression of the DBS construct abrogates recruitment of dynein to the cortex. *Insets* are shown *below* at *increased magnification*. *Scale bars*, 25 μm. *D*, expression of NCAM180 in HeLa cells stably expressing DHC-GFP induces the recruitment of dynein to NCAM180 patches at the cortex (*arrows*); this cortical localization is not observed in untransfected control cells. *Scale bar*, 10 μm. *E*, microtubules project to the cell cortex and are transiently stabilized at NCAM patches localized to the cell surface in COS7 cells expressing NCAM180 (*red*, RFP-NCAM180; *green*, GFP-EMTB, a microtubule-associated protein used to report microtubule dynamics). *F*, live cell imaging of microtubule dynamics in COS7 cells expressing NCAM180 (see supplemental Videos 1–3). An initial *two-color image* (*red*, RFP-NCAM180; *green*, GFP-EMTB) shows the tethering of a microtubule plus-end at an NCAM180 patch (*left*). A time series shows the tethering over time of the microtubule plus-end (*white dot*) at a cortical NCAM180 patch (*outlined* in *red*) in COS7 cells. Note the robust dynamics of untethered microtubules (*colored dots* and *lines*) within the same cell; *lines* indicate microtubule tracks over time, and *dots* indicate the initial position. *G*, microtubule tip trajectories away from (*left*) and at NCAM patches (*right*) show the dampened dynamics characteristic of tethered microtubules. Trajectories are aligned such that the initial microtubule tip position is at the origin. *H*, dampening of microtubule tip dynamics at NCAM patches. Tracking the tip positions over time of microtubules away from (*blue* and *green tracks*, *top*) and in NCAM patches (*red*, *yellow*, and *orange tracks*, *bottom*) shows the altered dynamics of microtubule growth and shortening of tethered microtubules. *Dots*, time points where the microtubule tip was localized in an NCAM patch. *I*, histogram of the microtubule tip velocities at (*red*) and away from (*blue*) NCAM180 patches at the cortex. The *inset* shows the mean and 25 and 75% quartiles of the absolute values of the velocity of the microtubule plus-ends ($p < 0.05$; ANOVA).

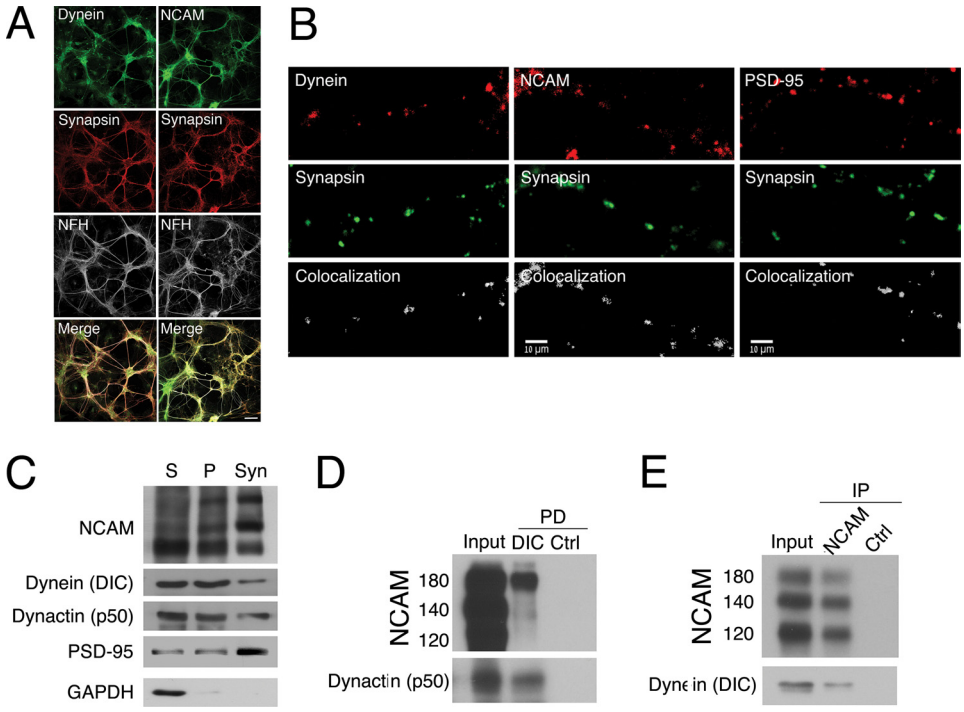

FIGURE 4. **Dynein and NCAM both localize to synaptic sites and co-precipitate from synaptosomal fractions.** *A*, dynein (*green*, *left*) and NCAM (*green*, *right*) localize with synapsin (*red*) in cortical neurons in contrast to neurofilament-H staining. *Scale bar*, 50 μm. *B*, dynein (*red*, *left*) and NCAM (*red*, *center*) both localize to synaptic sites along with the presynaptic marker synapsin shown in *green*, in the processes of cortical neurons at 14 DIV. The colocalization of postsynaptic marker PSD-95 (*red*, *panels* on *right*) with synapsin (*green*) is shown for comparison. *Scale bar*, 10 μm. The percentage of colocalization was determined from thresholded pre- and postsynaptic images using Imaris software (41); representative signals are shown (*Colocalization*) for each pair *below* the immunostained images. *C*, NCAM and dynein co-purify with synaptosomes. All three major NCAM isoforms (NCAM180, -140, and -120) were found in isolated synaptosomes, along with dynein (*DIC*) and dynactin (*p50*). Supernatant (*S*) and pellet (*P*) fractions from brain homogenate and the synaptosome-enriched fraction (*Syn*) were probed for the postsynaptic marker PSD-95, which is selectively enriched in the synaptosome fraction, and the cytosolic marker GAPDH, which is depleted. *D* and *E*, pull-down experiments from mouse brain synaptosomes show that NCAM180 is precipitated by recombinant DIC-bound beads (*D*) and that endogenous dynein is co-immunoprecipitated with NCAM antibodies (*E*).

ing microtubule plus-ends. This tethering correlates with enhanced cell-cell adhesion. Because NCAM180 is expressed specifically in neurons, we asked whether the dynein-NCAM180 interaction might have a role in regulating microtubule dynamics and enhancing cell-cell interactions in these cells.

To test this hypothesis, we first confirmed that NCAM and dynein both localize to synaptic sites in primary cortical neurons, as defined by colocalization with the synaptic marker synapsin (Fig. 4, *A* and *B*); the observed extent of colocalization for both dynein and NCAM was similar to that observed between the presynaptic marker synapsin and the postsynaptic marker PSD-95, whereas colocalization of neurofilaments and synapsin was over 3-fold lower ($p < 0.05$). Next, we isolated a synaptosomally enriched fraction from mouse brain and found that NCAM, dynein, and dynactin are all present in this preparation along with the synaptosomal marker PSD-95 (Fig. 4*C*). We then performed pull-down experiments from this synaptosomally enriched fraction. A pull-down experiment with recombinant DIC bound to beads shows that the NCAM180 isoform, but not the 140- or 120-kDa isoform, was co-precipitated from the synaptosomal fraction (Fig. 4*D*); dynactin (p50) served as a positive control. In the reciprocal experiment, endogenous dynein was co-immunoprecipitated from the synaptosomal fraction with an anti-NCAM antibody (Fig. 4*E*). Together, these observations led us to hypothesize that the dynein-NCAM interaction might have a functional role at synapses.

To examine the role of the dynein-NCAM interaction, we examined microtubule plus-end dynamics at synapses formed by cortical neurons in culture. We transfected primary cortical neurons with a plasmid encoding the microtubule plus-end tracking protein EB3 fused with mCherry and imaged microtubule dynamics in live cell assays (Fig. 5, *A* and *B*). We found that EB3-mCherry comets preferentially terminated at synaptic sites labeled with GFP-synaptophysin, ~2.5 times as often as would be expected if EB3 comets terminated at random sites along the neuronal process. EB3 associates only with actively growing microtubule ends, so we cannot distinguish if the EB3 signal is lost due to either preferential microtubule stabilization or catastrophe, and use of a general microtubule reporter construct like the EMTB construct used in COS7 cells did not provide sufficient resolution to monitor microtubule dynamics at the spatially restricted synapses formed by cortical neurons grown *in vitro*. However, the preferential termination of EB3 comets at synaptic sites is consistent with microtubule pausing induced by tethering, much as we observed in COS7 cells, which permit higher resolution imaging of microtubule dynamics.

To disrupt the NCAM180-dynein interaction, we used overexpression of the DBS of NCAM180, which, as shown above, acts as a dose-dependent inhibitor to block the dynein-NCAM interaction without perturbing other dynein functions in the cell (Fig. 1, *F* and *G*) (data not shown). In contrast to our observations in control neurons, the preferential termination of EB3

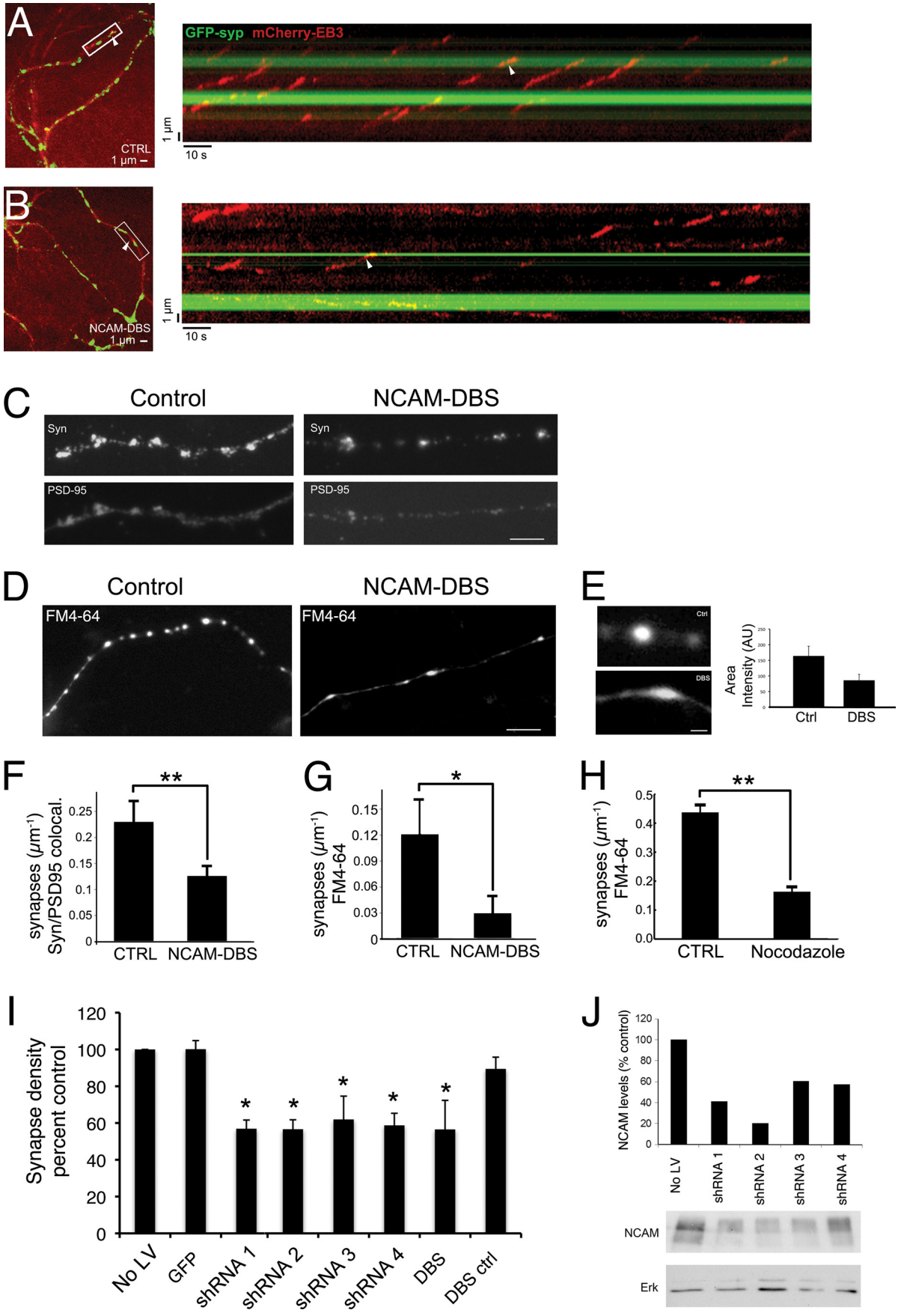
A
CTRL
1 μm
GFP-syp mCherry-EB3
1 μm
10 s
B
NCAM-DBS
1 μm
1 μm
10 s
C
Control
NCAM-DBS
Syn
PSD-95
D
Control
NCAM-DBS
FM4-64
E
Ctrl
DBS
Area Intensity (AU)
Ctrl
DBS
F
synapses (μm⁻¹) Syn/PSD95 colocal.
CTRL
NCAM-DBS
G
synapses (μm⁻¹) FM4-64
CTRL
NCAM-DBS
H
synapses (μm⁻¹) FM4-64
CTRL
Nocodazole
I
Synapse density percent control
No LV
GFP
shRNA 1
shRNA 2
shRNA 3
shRNA 4
DBS
DBS ctrl
J
NCAM levels (% control)
No LV
shRNA 1
shRNA 2
shRNA 3
shRNA 4
NCAM
Erk

comets at GFP-synaptophysin-positive sites was lost in neurons expressing the NCAM-DBS dominant negative construct (Fig. 5*B*). When the dynein-NCAM180 interaction is disrupted, EB3 comets terminated at apparently random locations along the neuron, because the fraction of EB3 comets terminating at synaptic sites is approximately equal to the fraction of the length of the neuron positive for the synaptic marker GFP-synaptophysin, as evidenced by the fraction of EB3 comets that terminate at synapses normalized to the fraction of the neurite length positive for GFP-synaptophysin (1.04 ± 1.04 for NCAM-DBS expressing neurons compared with 2.48 ± 0.52 for control neurons, mean ± S.E.).

As a further control to ensure that expression of the DBS did not affect overall microtubule dynamics in transfected cortical neurons, we analyzed both the velocity and the duration of EB3 comets along the processes and found that both aspects were similar in control neurons and those expressing DBS. The velocities in control and DBS-expressing neurons were 151 ± 9 and 135 ± 8 nm/s (mean ± S.E., $p > 0.2$), respectively. The apparent catastrophe frequencies (reciprocal of the duration of EB3 comets) also did not differ; means were 0.055 ± 0.008 and 0.067 ± 0.009 s^{-1} (±S.E.; $p > 0.4$; p values calculated by one-way ANOVA tests). These data suggest that the primary effect of DBS expression is disruption of the dynein-NCAM180 interaction rather than a direct effect on microtubule dynamics.

Disruption of the Dynein-NCAM180 Interaction Leads to Decreased Synaptic Density—The observation that EB3 comets preferentially terminate at synaptic sites is consistent with microtubule tethering and suggests that microtubule plus-ends tethered by NCAM180 and dynein may enhance cell-cell adhesion and thus synaptic stability. To test this hypothesis, we used the dominant negative DBS construct to disrupt the dynein-NCAM180 interaction in cortical neurons and then stained these neurons with antibodies to pre- and postsynaptic markers (Fig. 5*C*). Comparison of DBS-expressing neurons with control neurons indicated significantly fewer (0.13 ± 0.02; $p < 0.01$) synapses/μm in neurons expressing the inhibitory DBS construct as compared with control neurons (0.23 ± 0.03 synapses/μm; Fig. 5, *C* and *F*). In a complementary approach, we also analyzed the effects of DBS expression on the density of synapses measured by uptake of the fluorescent reporter FM4-64 following stimulation of the neurons with KCl (Fig. 5, *D* and *G*). We found that expression of DBS significantly decreased the density of active synapses (0.03 ± 0.02 synapses/μm as compared with 0.12 ± 0.04 synapses/μm in control neurons. We also noted that the FM4-64 staining of synapses in KCl-stimulated cortical neurons expressing the DBS construct was both less intense and less compact than in control neurons (Fig. 5*E*). Importantly, under these same conditions, we did not observe an effect of DBS expression on the dynein-mediated transport of either late endosomes/lysosomes or the synaptic marker GFP-Bsn along neuronal processes, indicating that DBS expression is not broadly inhibiting other dynein-mediated functions in the neuron.

Based on the hypothesis that the stabilization of synapses by the dynein-NCAM180 interaction is mediated by the tethering of microtubules to synaptic sites by dynein, we would predict that perturbing microtubule dynamics would also result in the loss of synaptic density. We used low dose nocodazole treatment to dampen microtubule dynamics without depolymerizing the microtubule cytoskeleton (45, 46). As expected, this treatment led to the loss of EB3-mCherry-positive comet tails. Cortical neurons treated with low dose nocodazole (50 nM for 20 h) exhibited decreased synaptic density (0.16 ± 0.01 synapses/μm, $p < 0.01$) as compared with control neurons (0.44 ± 0.03 synapses/μm; Fig. 5*H*), indicating that the maintenance of synaptic density requires dynamic microtubule remodeling.

Finally, we asked whether depletion of NCAM from cortical neurons induced a decrease in synaptic density similar to that induced by expression of the DBS construct blocking the dynein-NCAM180 interaction. We used four independent shRNA constructs expressed in lentivirus to deplete endogenous NCAM from cortical neurons (Fig. 5, *I* and *J*). Each of the four constructs led to marked loss of synaptic density, as assessed by the colocalization of pre- and postsynaptic markers (Fig. 5*I*); this loss was not observed in control neurons infected with lentivirus expressing GFP. Importantly, the synaptic loss observed upon depletion of NCAM was similar in magnitude to the decreased synaptic density induced by expression of the dominant negative DBS reagent (Fig. 5, *F*, *G*, and *I*).

FIGURE 5. **Inhibition of the dynein-NCAM180 interaction disrupts microtubule dynamics and decreases synaptic density in primary cortical neurons.** *A*, microtubule dynamics at synapses. Cortical neurons were transfected with EB3-mCherry and GFP-synaptophysin to image microtubule dynamics and synaptic sites. Shown in the *left panel* is a representative image from a single time point, and shown on the *right* is a kymograph generated from a line drawn along a neuronal process in the time series. A *white arrowhead* denotes the same representative EB3 comet in both the micrograph and the kymograph. These data show that EB3 comets preferentially terminate at synaptic sites in control neurons. *B*, expression of DBS alters microtubule dynamics at synapses. In neurons expressing the DBS from NCAM180, EB3 comets no longer terminate preferentially at synaptic sites. A representative micrograph is shown on the *left*, and a kymograph from the time series is shown on the *right*, with the same comet tail indicated in *both panels* by a *white arrowhead*. Expression of the NCAM-DBS domain reduces the fraction of EB3 comets terminating at synapses ($n > 85$ comets in >7 neurons). *C*, expression of the DBS from NCAM180 reduces synaptic density in cortical neurons, as assessed by colocalization of puncta positive for both pre- and postsynaptic markers (synapsin (*top*) and PSD-95 (*bottom*)). *D*, expression of the DBS from NCAM180 reduces synaptic density in cortical neurons as assessed by measuring KCl-stimulated uptake of FM4-64. *E*, expression of the NCAM-DBS in cortical neurons disrupts the appearance of FM4-64-positive synaptic sites. Synapses from cortical neurons transfected with the DBS from NCAM180 have a decreased area intensity (*DBS*; 86 ± 19 arbitrary units (*A.U.*)) compared with control neurons (*Ctrl*; 164 ± 31 arbitrary units, $p < 0.05$). Synapses in DBS-transfected neurons are also more broad, 2.4 ± 0.6 μm compared with 1.8 ± 0.4 μm in control neurons (*FWHM*; $p < 0.05$). *F* and *G*, quantitative decreases in synaptic density induced by expression of DBS assessed using either colocalization of pre- and postsynaptic markers ($p < 0.01$, $n = 15$ neurons with >1000 synapses from three experiments; *error bars*, S.E.) (*F*) or FM4-64 uptake ($p < 0.01$, $n = 18$ neurons with >1000 synapses from six experiments) (*G*). *H*, dampening microtubule dynamics decreased synaptic density. The effects of DBS expression on synaptic density can be compared with the effects of treatment of cortical neurons with low dose nocodazole (50 nM for 20 h) ($p < 0.01$, $n = 27$ neurons with >500 synapses from two experiments). Experimental values were measured relative to same day controls because synaptic density is dependent on plating density and DIV. *I*, depletion of NCAM using four different shRNA (*shRNA 1–4*) constructs or expression of the dominant negative DBS construct resulted in similar decreases in synaptic density, relative to controls (*NO LV*, no lentivirus infection; *GFP*, infection with lentivirus expressing GFP; *DBS ctrl*, mock transfection). For all *panels*, *, $p < 0.05$; **, $p < 0.01$. *J*, depletion of NCAM isoforms from cortical neuronal cultures by lentivirus expression of shRNA constructs targeting NCAM as assessed by Western blot; ERK immunoreactivity was used as a loading control.

DISCUSSION

Dynein has been primarily characterized in neurons as the major microtubule motor driving retrograde transport of intracellular cargos. However, increasing evidence suggests that dynein also has important functions at the cell cortex. During mitosis, cortically localized dynein acts to position the mitotic spindle (8, 10). Dynein is also specifically recruited to cortical sites in interphase cells, including epithelial adherens junctions (11, 12) and the immunological synapse (13). Recent biophysical studies have shown that dynein at the cortex is uniquely suited to tethering dynamic microtubule plus-ends. In reconstitution assays with dynein bound either to beads or to microfabricated barriers, dynamic microtubule plus-ends made stable contacts with the barrier. In contrast, encounters between microtubules and barriers in the absence of dynein led to rapid catastrophe (14, 15, 47).

Here, we describe a direct and specific interaction between cytoplasmic dynein and the neural cell adhesion molecule NCAM180. Heterologous expression of NCAM180 in COS7 or HeLa cells leads to the recruitment of dynein to NCAM180-positive patches at the cell cortex. In live cell assays, we observe that microtubule plus-ends projecting toward these NCAM180 patches are transiently stabilized. In primary neurons, we find that inhibition of the dynein-NCAM180 interaction or depletion of NCAM perturbs microtubule dynamics at synaptic sites and results in a significant loss of synaptic density. Based on our experimental observations, we propose the following hypothesis. Dynein, anchored to the cortex at synaptic sites through a direct association with NCAM180, tethers microtubule plus-ends. The microtubule-dynein-NCAM180 interaction may contribute to the stability of intercellular interactions at synaptic sites, consistent with our observation of decreased synaptic density in neurons in which this interaction is blocked. Interestingly, the decreased synaptic density observed upon inhibition of the dynein-NCAM180 interaction or upon depletion of NCAM from the neuron parallels the decreased density induced by treating cortical neurons with low dose nocodazole, which dampens microtubule dynamics and hinders their ability to search cellular space.

NCAM180 is an adhesion molecule that is localized to synapses and contributes to synaptic stabilization and maturation (20, 21, 27, 48). NCAM180 is involved in the localized accumulation of synaptic organelles and proteins (26). Studies in knock-out mice indicate that loss of NCAM180 expression affects synapse maturation and stability (20, 21, 27, 48), including junctional stability in neurons following injury (24). NCAM180 knock-out mice exhibit periods of complete transmission failure upon repetitive stimulation of the neuromuscular junction (NMJ) (21, 22, 27). NCAM-deficient mice also exhibit impaired long term potentiation (49), suggestive of a possible defect in cytoskeletal remodeling at synaptic sites.

Previous studies have also implicated dynein and dynactin in the maintenance of synaptic stability. In *Drosophila*, depletion of dynactin leads to synaptic retraction and destabilization of the NMJ (50). Destabilization and loss of NMJs have been observed in dynein mutant mice (51). Also consistent with a role for dynein-dynactin in maintaining the stability of the NMJ, analysis of a transgenic mouse model expressing the G59S mutation in dynactin causative for human motor neuron disease (HMN7B) has shown significant synaptic destabilization in the absence of marked defects in axonal transport (52). Of note, the long term potentiation impairment observed in NCAM-deficient mice shows a pronounced age-dependent decline, whereas dynactin mutant (Glued) flies exhibit both morphological and functional deficits that increase with age (53).

Recent work has begun to explore the role of microtubule dynamics at synapses (reviewed in Ref. 54). Studies in *Drosophila* clearly implicate proteins modulating microtubule dynamics in the regulation of synaptic morphology and stability (55–58). In mammalian neurons, EM analysis shows microtubules at neuromuscular junctions (59–61), and, more recently, the observation of microtubule invasions of dendritic spines (62–65) has suggested a role for microtubules in modulating synaptic plasticity. A specific role for microtubule plus-end dynamics in either the establishment or maintenance of synaptic morphology was suggested by recent work on the plus-end tracking protein CLASP2. Knockdown of CLASP2 in hippocampal neurons led to a decrease in synaptic density and synaptic area (66), similar to the alterations induced here by blocking the dynein-NCAM180 interaction or depleting NCAM from cortical neurons.

How might dynein-mediated microtubule tethering affect synaptic morphology or function? There are a number of possible models. Dynein-mediated microtubule tethering may contribute to the regulation of microtubule dynamics at synaptic sites. Dynein-mediated microtubule tethering may also facilitate the spatially specific trafficking of vesicles to the synapse, because cortically tethered microtubules have been proposed to serve as preferred tracks for rapid communication from the cell center to the periphery (67). Alternatively, a link between the internal microtubule cytoskeleton and sites of cell-cell interaction may also provide mechanical stability. The extracellular domain of NCAM is involved in molecular interactions between the pre- and postsynaptic compartments. Thus, microtubules tethered by dynein may provide a physical link between the extracellular milieu and the cytoskeleton that is able to exert force. In a mechanosensory role, the dynein-NCAM interaction could serve to "report" the physical properties of the surrounding environment in a transmembrane feedback mechanism, as has been suggested in studies on apCAM at *Aplysia* growth cones (68). Further studies, using superresolution microscopy and electrophysiology, will be required to discriminate among these models.

NCAM180 may not be the only adhesion molecule that can recruit dynein to the cortex; a direct interaction between dynein and β-catenin (12) may provide some functional redundancy at the synapse where β-catenin is also localized (69). Consistent with this hypothesis, ablation of NCAM expression results in pleiotropic effects on the nervous system (18) but is not lethal, in contrast to loss of dynein or dynactin expression (70). Also, our work does not rule out other key interactions between NCAM and the cellular cytoskeleton. Polo-Parada *et al.* (71) have previously described a conserved C-terminal motif in NCAM that may signal via myosin light chain kinase to reg-

ulate myosin-driven synaptic vesicle trafficking at the presynaptic terminal. At the postsynaptic terminal, an association with a spectrin-based scaffold mediates the accumulation of NCAM at synaptic contacts (23, 72). Dynein has also been shown to interact indirectly with the spectrin cytoskeleton via dynactin (35) and ankyrin (73), so multiple interactions probably contribute to dynamically link the cytoskeleton to the cell cortex at active trafficking sites, such as synapses. Together, these observations suggest that regulated interactions between the cellular cytoskeleton and the cell cortex play a key role in maintaining the stability and function of neurons.

REFERENCES

1. Kardon, J. R., and Vale, R. D. (2009) Regulators of the cytoplasmic dynein motor. *Nat. Rev. Mol. Cell Biol.* **10,** 854–865
2. Nyarko, A., Song, Y., and Barbar, E. (2012) Intrinsic disorder in dynein intermediate chain modulates its interactions with NudE and dynactin. *J. Biol. Chem.* **287,** 24884–24893
3. Kirschner, M., and Mitchison, T. (1986) Beyond self-assembly. From microtubules to morphogenesis. *Cell* **45,** 329–342
4. Levy, J. R., and Holzbaur, E. L. (2007) Special delivery. Dynamic targeting via cortical capture of microtubules. *Dev. Cell* **12,** 320–322
5. Heil-Chapdelaine, R. A., Oberle, J. R., and Cooper, J. A. (2000) The cortical protein Num1p is essential for dynein-dependent interactions of microtubules with the cortex. *J. Cell Biol.* **151,** 1337–1344
6. Markus, S. M., and Lee, W. L. (2011) Regulated offloading of cytoplasmic dynein from microtubule plus ends to the cortex. *Dev. Cell* **20,** 639–651
7. Ten Hoopen, R., Cepeda-Garcia, C., Fernández-Arruti, R., Juanes, M. A., Delgehyr, N., and Segal, M. (2012) Mechanism for astral microtubule capture by cortical Bud6p priming spindle polarity in *S. cerevisiae*. *Curr. Biol.* **22,** 1075–1083
8. Moore, J. K., and Cooper, J. A. (2010) Coordinating mitosis with cell polarity. Molecular motors at the cell cortex. *Semin. Cell Dev. Biol.* **21,** 283–289
9. Gönczy, P. (2008) Mechanisms of asymmetric cell division. Flies and worms pave the way. *Nat. Rev. Mol. Cell Biol.* **9,** 355–366
10. Kiyomitsu, T., and Cheeseman, I. M. (2012) Chromosome- and spindle-pole-derived signals generate an intrinsic code for spindle position and orientation. *Nat. Cell Biol.* **14,** 311–317
11. Ligon, L. A., and Holzbaur, E. L. (2007) Microtubules tethered at epithelial cell junctions by dynein facilitate efficient junction assembly. *Traffic* **8,** 808–819
12. Ligon, L. A., Karki, S., Tokito, M., and Holzbaur, E. L. (2001) Dynein binds to β-catenin and may tether microtubules at adherens junctions. *Nat. Cell Biol.* **3,** 913–917
13. Combs, J., Kim, S. J., Tan, S., Ligon, L. A., Holzbaur, E. L., Kuhn, J., and Poenie, M. (2006) Recruitment of dynein to the Jurkat immunological synapse. *Proc. Natl. Acad. Sci. U.S.A.* **103,** 14883–14888
14. Hendricks, A. G., Lazarus, J. E., Perlson, E., Gardner, M. K., Odde, D. J., Goldman, Y. E., and Holzbaur, E. L. (2012) Dynein tethers and stabilizes dynamic microtubule plus ends. *Curr. Biol.* **22,** 632–637
15. Laan, L., Pavin, N., Husson, J., Romet-Lemonne, G., van Duijn, M., López, M. P., Vale, R. D., Jülicher, F., Reck-Peterson, S. L., and Dogterom, M. (2012) Cortical dynein controls microtubule dynamics to generate pulling forces that position microtubule asters. *Cell* **148,** 502–514
16. Persohn, E., Pollerberg, G. E., and Schachner, M. (1989) Immunoelectron-microscopic localization of the 180 kD component of the neural cell adhesion molecule N-CAM in postsynaptic membranes. *J. Comp. Neurol.* **288,** 92–100
17. Persohn, E., and Schachner, M. (1990) Immunohistological localization of the neural adhesion molecules L1 and N-CAM in the developing hippocampus of the mouse. *J. Neurocytol.* **19,** 807–819
18. Cremer, H., Lange, R., Christoph, A., Plomann, M., Vopper, G., Roes, J., Brown, R., Baldwin, S., Kraemer, P., and Scheff, S. (1994) Inactivation of the N-CAM gene in mice results in size reduction of the olfactory bulb and deficits in spatial learning. *Nature* **367,** 455–459
19. Muller, D., Wang, C., Skibo, G., Toni, N., Cremer, H., Calaora, V., Rougon, G., and Kiss, J. Z. (1996) PSA-NCAM is required for activity-induced synaptic plasticity. *Neuron* **17,** 413–422
20. Dityatev, A., Dityateva, G., and Schachner, M. (2000) Synaptic strength as a function of post- *versus* presynaptic expression of the neural cell adhesion molecule NCAM. *Neuron* **26,** 207–217
21. Rafuse, V. F., Polo-Parada, L., and Landmesser, L. T. (2000) Structural and functional alterations of neuromuscular junctions in NCAM-deficient mice. *J. Neurosci.* **20,** 6529–6539
22. Polo-Parada, L., Bose, C. M., and Landmesser, L. T. (2001) Alterations in transmission, vesicle dynamics, and transmitter release machinery at NCAM-deficient neuromuscular junctions. *Neuron* **32,** 815–828
23. Sytnyk, V., Leshchyns'ka, I., Nikonenko, A. G., and Schachner, M. (2006) NCAM promotes assembly and activity-dependent remodeling of the postsynaptic signaling complex. *J. Cell Biol.* **174,** 1071–1085
24. Chipman, P. H., Franz, C. K., Nelson, A., Schachner, M., and Rafuse, V. F. (2010) Neural cell adhesion molecule is required for stability of reinnervated neuromuscular junctions. *Eur. J. Neurosci.* **31,** 238–249
25. Cunningham, B. A., Hemperly, J. J., Murray, B. A., Prediger, E. A., Brackenbury, R., and Edelman, G. M. (1987) Neural cell adhesion molecule. Structure, immunoglobulin-like domains, cell surface modulation, and alternative RNA splicing. *Science* **236,** 799–806
26. Maness, P. F., and Schachner, M. (2007) Neural recognition molecules of the immunoglobulin superfamily. Signaling transducers of axon guidance and neuronal migration. *Nat. Neurosci.* **10,** 19–26
27. Polo-Parada, L., Bose, C. M., Plattner, F., and Landmesser, L. T. (2004) Distinct roles of different neural cell adhesion molecule (NCAM) isoforms in synaptic maturation revealed by analysis of NCAM 180 kDa isoform-deficient mice. *J. Neurosci.* **24,** 1852–1864
28. Karki, S., and Holzbaur, E. L. (1995) Affinity chromatography demonstrates a direct binding between cytoplasmic dynein and the dynactin complex. *J. Biol. Chem.* **270,** 28806–28811
29. Moughamian, A. J., and Holzbaur, E. L. (2012) Dynactin is required for transport initiation from the distal axon. *Neuron* **74,** 331–343
30. Miller, P. M., Folkmann, A. W., Maia, A. R., Efimova, N., Efimov, A., and Kaverina, I. (2009) Golgi-derived CLASP-dependent microtubules control Golgi organization and polarized trafficking in motile cells. *Nat. Cell Biol.* **11,** 1069–1080
31. Faire, K., Waterman-Storer, C. M., Gruber, D., Masson, D., Salmon, E. D., and Bulinski, J. C. (1999) E-MAP-115 (ensconsin) associates dynamically with microtubules *in vivo* and is not a physiological modulator of microtubule dynamics. *J. Cell Sci.* **112,** 4243–4255
32. Fejtova, A., Davydova, D., Bischof, F., Lazarevic, V., Altrock, W. D., Romorini, S., Schöne, C., Zuschratter, W., Kreutz, M. R., Garner, C. C., Ziv, N. E., and Gundelfinger, E. D. (2009) Dynein light chain regulates axonal trafficking and synaptic levels of Bassoon. *J. Cell Biol.* **185,** 341–355
33. Toba, S., and Toyoshima, Y. Y. (2004) Dissociation of double-headed cytoplasmic dynein into single-headed species and its motile properties. *Cell Motil. Cytoskeleton* **58,** 281–289
34. Castoldi, M., and Popov, A. V. (2003) Purification of brain tubulin through two cycles of polymerization-depolymerization in a high-molarity buffer. *Protein Expr. Purif.* **32,** 83–88
35. Holleran, E. A., Ligon, L. A., Tokito, M., Stankewich, M. C., Morrow, J. S., and Holzbaur, E. L. (2001) β III spectrin binds to the Arp1 subunit of dynactin. *J. Biol. Chem.* **276,** 36598–36605
36. Perlson, E., Jeong, G. B., Ross, J. L., Dixit, R., Wallace, K. E., Kalb, R. G., and Holzbaur, E. L. (2009) A switch in retrograde signaling from survival to stress in rapid-onset neurodegeneration. *J. Neurosci.* **29,** 9903–9917
37. Dichter, M. A. (1978) Rat cortical neurons in cell culture. Culture methods, cell morphology, electrophysiology, and synapse formation. *Brain Res.* **149,** 279–293
38. Tiscornia, G., Singer, O., and Verma, I. M. (2006) Production and purification of lentiviral vectors. *Nat. Protoc.* **1,** 241–245
39. Hata, K., Polo-Parada, L., and Landmesser, L. T. (2007) Selective targeting of different neural cell adhesion molecule isoforms during motoneuron myotube synapse formation in culture and the switch from an immature to mature form of synaptic vesicle cycling. *J. Neurosci.* **27,** 14481–14493
40. Rogers, S. W., Hughes, T. E., Hollmann, M., Gasic, G. P., Deneris, E. S., and

Heinemann, S. (1991) The characterization and localization of the glutamate receptor subunit GluR1 in the rat brain. *J. Neurosci.* **11,** 2713–2724
41. Costes, S. V., Daelemans, D., Cho, E. H., Dobbin, Z., Pavlakis, G., and Lockett, S. (2004) Automatic and quantitative measurement of protein-protein colocalization in live cells. *Biophys. J.* **86,** 3993–4003
42. Maas, C., Tagnaouti, N., Loebrich, S., Behrend, B., Lappe-Siefke, C., and Kneussel, M. (2006) Neuronal cotransport of glycine receptor and the scaffold protein gephyrin. *J. Cell Biol.* **172,** 441–451
43. Teuling, E., van Dis, V., Wulf, P. S., Haasdijk, E. D., Akhmanova, A., Hoogenraad, C. C., and Jaarsma, D. (2008) A novel mouse model with impaired dynein/dynactin function develops amyotrophic lateral sclerosis (ALS)-like features in motor neurons and improves lifespan in SOD1-ALS mice. *Hum. Mol. Genet.* **17,** 2849–2862
44. Quintyne, N. J., Gill, S. R., Eckley, D. M., Crego, C. L., Compton, D. A., and Schroer, T. A. (1999) Dynactin is required for microtubule anchoring at centrosomes. *J. Cell Biol.* **147,** 321–334
45. Vasquez, R. J., Howell, B., Yvon, A. M., Wadsworth, P., and Cassimeris, L. (1997) Nanomolar concentrations of nocodazole alter microtubule dynamic instability in vivo and in vitro. *Mol. Biol. Cell* **8,** 973–985
46. Jaworski, J., Hoogenraad, C. C., and Akhmanova, A. (2008) Microtubule plus-end tracking proteins in differentiated mammalian cells. *Int. J. Biochem. Cell Biol.* **40,** 619–637
47. Janson, M. E., de Dood, M. E., and Dogterom, M. (2003) Dynamic instability of microtubules is regulated by force. *J. Cell Biol.* **161,** 1029–1034
48. Moscoso, L. M., Cremer, H., and Sanes, J. R. (1998) Organization and reorganization of neuromuscular junctions in mice lacking neural cell adhesion molecule, tenascin-C, or fibroblast growth factor-5. *J. Neurosci.* **18,** 1465–1477
49. Kochlamazashvili, G., Bukalo, O., Senkov, O., Salmen, B., Gerardy-Schahn, R., Engel, A. K., Schachner, M., and Dityatev, A. (2012) Restoration of synaptic plasticity and learning in young and aged NCAM-deficient mice by enhancing neurotransmission mediated by GluN2A-containing NMDA receptors. *J. Neurosci.* **32,** 2263–2275
50. Eaton, B. A., Fetter, R. D., and Davis, G. W. (2002) Dynactin is necessary for synapse stabilization. *Neuron* **34,** 729–741
51. Courchesne, S. L., Pazyra-Murphy, M. F., Lee, D. J., and Segal, R. A. (2011) Neuromuscular junction defects in mice with mutation of dynein heavy chain 1. *PLoS One* **6,** e16753
52. Chevalier-Larsen, E. S., Wallace, K. E., Pennise, C. R., and Holzbaur, E. L. (2008) Lysosomal proliferation and distal degeneration in motor neurons expressing the G59S mutation in the p150Glued subunit of dynactin. *Hum. Mol. Genet.* **17,** 1946–1955
53. Rawson, J. M., Kreko, T., Davison, H., Mahoney, R., Bokov, A., Chang, L., Gelfond, J., Macleod, G. T., and Eaton, B. A. (2012) Effects of diet on synaptic vesicle release in dynactin complex mutants. A mechanism for improved vitality during motor disease. *Aging Cell* **11,** 418–427
54. Goellner, B., and Aberle, H. (2012) The synaptic cytoskeleton in development and disease. *Dev. Neurobiol.* **72,** 111–125
55. Roos, J., Hummel, T., Ng, N., Klämbt, C., and Davis, G. W. (2000) *Drosophila* Futsch regulates synaptic microtubule organization and is necessary for synaptic growth. *Neuron* **26,** 371–382
56. Orso, G., Martinuzzi, A., Rossetto, M. G., Sartori, E., Feany, M., and Daga, A. (2005) Disease-related phenotypes in a *Drosophila* model of hereditary spastic paraplegia are ameliorated by treatment with vinblastine. *J. Clin. Invest.* **115,** 3026–3034
57. Graf, E. R., Heerssen, H. M., Wright, C. M., Davis, G. W., and DiAntonio, A. (2011) Stathmin is required for stability of the *Drosophila* neuromuscular junction. *J. Neurosci.* **31,** 15026–15034
58. Nahm, M., Lee, M. J., Parkinson, W., Lee, M., Kim, H., Kim, Y. J., Kim, S., Cho, Y. S., Min, B. M., Bae, Y. C., Broadie, K., and Lee, S. (2013) Spartin regulates synaptic growth and neuronal survival by inhibiting BMP-mediated microtubule stabilization. *Neuron* **77,** 680–695
59. Gray, E. G. (1975) Presynaptic microtubules and their association with synaptic vesicles. *Proc. R Soc. Lond. B Biol. Sci.* **190,** 367–372
60. Gray, E. G. (1976) Microtubules in synapses of the retina. *J. Neurocytol.* **5,** 361–370
61. Gray, E. G. (1978) Synaptic vesicles and microtubules in frog motor endplates. *Proc. R. Soc. Lond. B Biol. Sci.* **203,** 219–227
62. Gu, J., Firestein, B. L., and Zheng, J. Q. (2008) Microtubules in dendritic spine development. *J. Neurosci.* **28,** 12120–12124
63. Hu, X., Viesselmann, C., Nam, S., Merriam, E., and Dent, E. W. (2008) Activity-dependent dynamic microtubule invasion of dendritic spines. *J. Neurosci.* **28,** 13094–13105
64. Jaworski, J., Kapitein, L. C., Gouveia, S. M., Dortland, B. R., Wulf, P. S., Grigoriev, I., Camera, P., Spangler, S. A., Di Stefano, P., Demmers, J., Krugers, H., Defilippi, P., Akhmanova, A., and Hoogenraad, C. C. (2009) Dynamic microtubules regulate dendritic spine morphology and synaptic plasticity. *Neuron* **61,** 85–100
65. Merriam, E. B., Lumbard, D. C., Viesselmann, C., Ballweg, J., Stevenson, M., Pietila, L., Hu, X., and Dent, E. W. (2011) Dynamic microtubules promote synaptic NMDA receptor-dependent spine enlargement. *PLoS One* **6,** e27688
66. Beffert, U., Dillon, G. M., Sullivan, J. M., Stuart, C. E., Gilbert, J. P., Kambouris, J. A., and Ho, A. (2012) Microtubule plus-end tracking protein CLASP2 regulates neuronal polarity and synaptic function. *J. Neurosci.* **32,** 13906–13916
67. Kaverina, I., Krylyshkina, O., and Small, J. V. (1999) Microtubule targeting of substrate contacts promotes their relaxation and dissociation. *J. Cell Biol.* **146,** 1033–1044
68. Suter, D. M., Errante, L. D., Belotserkovsky, V., and Forscher, P. (1998) The Ig superfamily cell adhesion molecule, apCAM, mediates growth cone steering by substrate-cytoskeletal coupling. *J. Cell Biol.* **141,** 227–240
69. Tanaka, H., Takafuji, K., Taguchi, A., Wiriyasermkul, P., Ohgaki, R., Nagamori, S., Suh, P. G., and Kanai, Y. (2012) Linkage of N-cadherin to multiple cytoskeletal elements revealed by a proteomic approach in hippocampal neurons. *Neurochem. Int.* **61,** 240–250
70. Perlson, E., Maday, S., Fu, M. M., Moughamian, A. J., and Holzbaur, E. L. (2010) Retrograde axonal transport. Pathways to cell death? *Trends Neurosci.* **33,** 335–344
71. Polo-Parada, L., Plattner, F., Bose, C., and Landmesser, L. T. (2005) NCAM 180 acting via a conserved C-terminal domain and MLCK is essential for effective transmission with repetitive stimulation. *Neuron* **46,** 917–931
72. Leshchyns'ka, I., Tanaka, M. M., Schachner, M., and Sytnyk, V. (2011) Immobilized pool of NCAM180 in the postsynaptic membrane is homeostatically replenished by the flux of NCAM180 from extrasynaptic regions. *J. Biol. Chem.* **286,** 23397–23406
73. Ayalon, G., Davis, J. Q., Scotland, P. B., and Bennett, V. (2008) An ankyrin-based mechanism for functional organization of dystrophin and dystroglycan. *Cell* **135,** 1189–1200